Penta-PdX_2 (X = S, Se, Te) monolayers: promising anisotropic thermoelectric materials

Yang-Shun Lan [1], Xiang-Rong Chen [1], Cui-E Hu [2, *], Yan Cheng [1, *], Qi-Feng Chen [3]

[1] College of Physical Science and Technology, Sichuan University, Chengdu 610065, China;

[2] College of Physics and Electronic Engineering, Chongqing Normal University, Chongqing 400047, China;

[3] National Key Laboratory for Shock Wave and Detonation Physics Research, Institute of Fluid Physics, Chinese Academy of Engineering Physics, Mianyang 621900, China

Abstract: Thermoelectric materials can be used to convert waste heat into electrical energy, which is considered to be a cleaner form of energy that reduces carbon dioxide and greenhouse gas emissions. In this work, we study the thermoelectric properties of penta-PdX_2 (X = S, Se, Te) using first-principles calculations together with the Boltzmann transport theory. The dynamic and thermal stability of penta-PdX_2 is confirmed based on phonon dispersion and *ab initio* molecular dynamics (AIMD) simulations. The transport coefficients, such as thermal conductivity (k_l), power factor (*PF*) and thermoelectric figure of merit (*ZT*), exhibit strong anisotropy in both *x* and *y* directions. The lower thermal conductivity of penta-PdX_2 can be attributed to the lower group velocity and larger phase space. The thermal conductivity of penta-PdX_2 along the same direction (*x* or *y* direction) adheres to a trend of PdS_2 > $PdSe_2$ > $PdTe_2$. The anisotropy of *PF* and k_l of penta-PdX_2 monolayer inevitably leads to anisotropy of *ZT*.

[*] *Corresponding authors. E-mail: cuiehu@126.com; ycheng@scu.edu.cn*

The largest *ZT* values of penta-PdX2 (X = S, Se) at p-type are 0.85 and 1.18 respectively, while the maximum *ZT* value of penta-PdTe2 has reached 2.42. The predicted *ZT* value in penta-PdX_2 are larger than the commercial TE material Bi_2Te_3 (about 0.8) and some other transition metal di-chalcogenides, indicating that penta-PdX_2 (X = S, Se, Te) monolayer is a potential anisotropic thermoelectric material.

Key words: Pentagonal structure; First-principles investigations; Thermal transport; Thermoelectric material

Table S1. Calculated effective mass (m^*), average effective mass (m_d), elastic modulus (C_{2D}), deformation potential constant (E_1), carrier mobility (μ) and relaxation time (τ) of penta-PdX_2 (X = S, Se, Te) monolayers at 300 K along the *x* and *y* directions.

	directions	carriers	m^* (m_e)	m_d(m_e)	C_{2D} (eV/Å^2)	E_l(eV)	μ (cm^{2}V^{-1}s^{-1})	τ (10^{-14} s)
PdS_2	*x*	e	0.82	0.48	3.54	-8.80	39.40	1.83
		h	0.46	0.83	3.54	-1.37	1664.15	43.61
	y	e	0.28	0.48	4.89	-9.36	137.49	2.23
		h	1.49	0.83	4.89	-1.46	631.94	53.46
$PdSe_2$	*x*	e	0.33	0.20	2.36	-8.15	177.13	3.33
		h	0.36	0.25	2.36	-2.40	1485.92	30.84
	y	e	0.12	0.20	3.85	-8.85	630.21	4.61
		h	0.18	0.25	3.85	-2.67	3997.68	40.81
$PdTe_2$	*x*	e	0.35	0.32	1.44	-4.01	268.55	5.38
		h	0.16	0.12	1.44	-2.84	2924.89	26.97
	y	e	0.29	0.32	3.19	-4.55	545.75	9.21
		h	0.10	0.13	3.19	-3.34	7454.75	57.88

Table S2. The optimized lattice parameters (*a*, *b*), length of Pd-S ($d_{Pd\text{-}S}$) and S-S ($d_{S\text{-}S}$) bonds, and band gap (E_{gp}) of the penta-PdX_2 (X = S, Se, Te) monolayers.

	result	*a* (Å)	*b* (Å)	$d_{Pd\text{-}S}$ (Å)	$d_{S\text{-}S}$ (Å)	E_{gp} (eV)
PdS_2	Present	5.48	5.57	2.33,2.34	2.09	1.14(PBE), 2.12(HSE)
	Exp.	5.41	5.49	-	-	-
	Wang *et al.*	5.49	5.59	2.34,2.35	2.10	1.60(HSE)
	Deng *et al.*	5.50	5.59	-	-	1.00(PBE)
$PdSe_2$	Present	5.74	5.91	2.45,2.46	2.41	1.34(PBE), 2.14(HSE)
	Exp.	5.74	5.86	-	-	-
	Deng *et al.*	5.49	5.94	-	-	1.31(PBE)
	Qin *et al.*	5.75	5.92	-	-	1.38(PBE)
	Oyedele *et al.*	5.72	5.93	-	-	-
$PdTe_2$	Present	6.14	6.44	2.62,2.63	2.80	1.24(PBE),1.84(HSE)
	Deng *et al.*	5.99	6.37	-	-	-

Table S3. Contribution rates of penta-PdX_2 acoustical phonon branches (ZA, TA, LA) and optical phonons support to thermal conductance at 300 K.

	directions	ZA	TA	LA	optical
PdS_2	*x*	13.57%	28.17%	45.03%	13.23%
	y	36.37%	12.47%	44.81%	6.35%
$PdSe_2$	*x*	27.97%	33.22%	17.29%	21.52%
	y	40.30%	27.02%	20.97%	11.71%
$PdTe_2$	*x*	27.74%	18.84%	35.10%	18.32%
	y	49.86%	19.13%	24.17%	6.84%

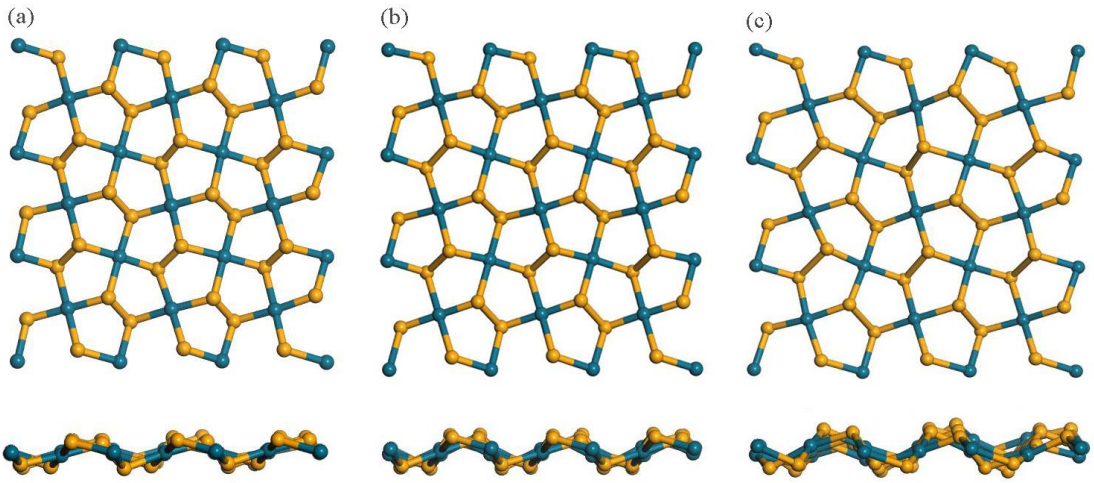

Fig. S1 Snapshot of AIMD simulations at 300 K for (a) penta-PdS_2, (b) penta-$PdSe_2$, and (c) penta-$PdTe_2$ monolayers, respectively.

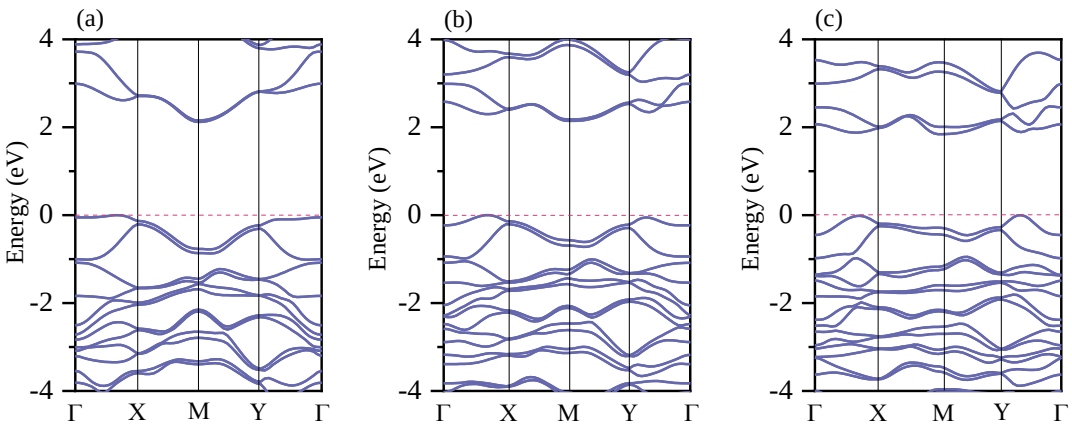

Fig. S2 HSE band structures with SOC for (a) penta-PdS_2, (b) penta-$PdSe_2$ and (c) penta-$PdTe_2$ monolayers, respectively.

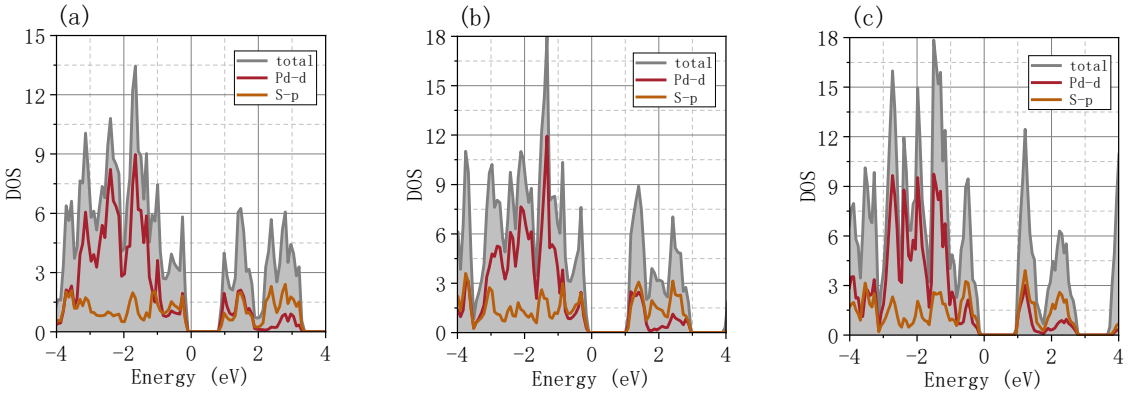

Fig. S3 Total and partial density of states of (a) penta-PdS_2, (b) penta-$PdSe_2$ and (c) penta-$PdTe_2$ monolayers.

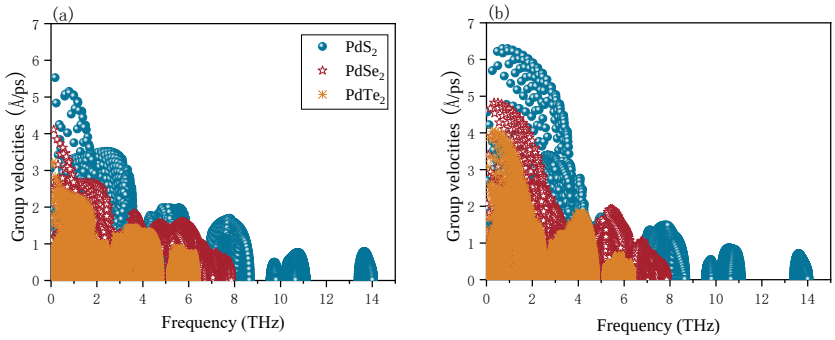

Fig.S4 Frequency-dependent group velocity of penta-PdX_2 (X = S, Se, Te) monolayers along x (a) and y (b) direction.

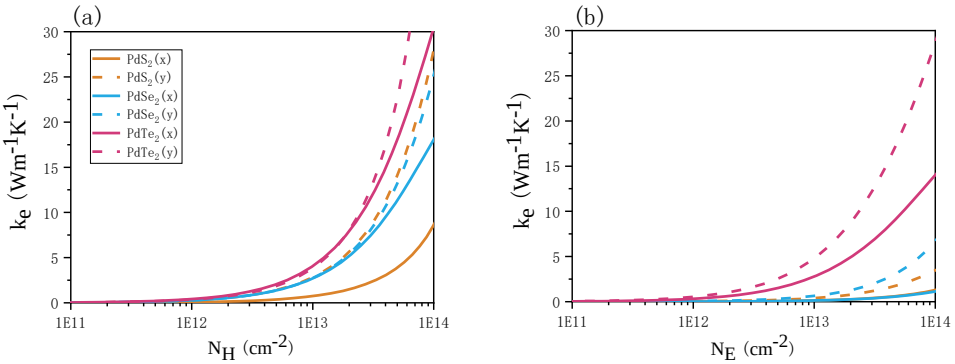

Fig. S5 The electronic thermal conductivity (k_e) of penta-PdX_2 (X = S, Se, Te) monolayers for both *p*-type (a) and *n*-type (b) at 300 K along the *x* (solid lines) and y (dotted lines) directions.